Asteroseismology of Solar-Like Stars

Engin Keen *, Thomas North †, Ditte Slumstrup ‡

November 19, 2014

Abstract

In this work we use photometric data from Kepler space observatory of 10 main sequence stars and one red giant star to determine the mass, radius, luminosity and age of these stars. We identify the different p-mode oscillations of these stars from a Fourier transform of the time series and determine by hand the large frequency separation, $\Delta\nu$, and the small frequency separation, $\delta\nu$. With this we determined the mass and age of the stars using a so called C-D-diagram and thereafter plot the stars in a Hertzsprung-Russell-diagram. Results were compared to literature source and good agreement within 1% for the $\Delta\nu$ was found.

Introduction

Stars have fascinated humanity as long as humans have existed, and not only their beauty makes them unique. And of course, one should look always to the "inner beauty". But what does this means in the case of stars? Stars pulsates through heating and cooling, they contract and expand. This leads to change in brightness of the star, which can be measured. This allows for the deduction of the properties of stars. This is called asteroseismology.

The ultimate goal of asteroseismology is to detect enough stellar oscillation frequencies for different modes so that the interior sound speed can be mapped and deductions can be made about temperature, pressure, mass, age, rotation and internal structre of the star.

The understanding behind oscillations within stars has increased dramatically over the past two decades due to extensive research of the excellent data provided by recent space-based missions. The most recent of these missions is the Kepler mission which has provided excellent photometric data on many stars. There is now hope that the upcoming TESS mission can provide data on tens of thousands of stars for asteroseismic research.

In this work, we analysed 10 main sequence solar-like stars and one red giant star. For these stars, Kepler short cadence data will be used. We will determine the mass, radius and the age of these stars.

*email:
†email:TXN016@bham.ac.uk
‡email: ds09@phys.au.dk

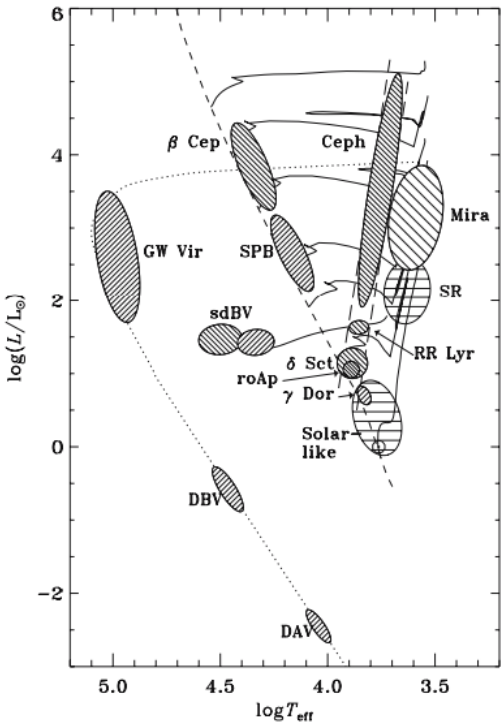

Figure 1: *Hertzsprung-Russell diagram showing different possible stellar oscillations. The main sequence is represented by the dashed line. As can be seen solar like oscillations (dashed areas) represent an area where the instability strip and main sequence intersect on a HR diagram.*[8]

Pulsating Intrinsic Variables

Stars that have time-dependent fluctuations in apparent magnitude on time scales smaller than that of evolutionary time scales, are classed as variable stars. Asteroseismology is the study of oscillations within pulsating intrinsic variable stars, where intrinsic means that the luminosity variations of the star are caused by changes in the stellar interior. Stars are in hydrostatic equilibrium, a balance between the gravitational and pressure gradient forces, and as a result, any perturbation will be damped by some restoring force. Therefore, for an oscillation to propagate within the interior, it requires a driving mechanism. There are four major mechanisms that drive oscillations within stars, each of which vary depending on the properties of that star. For the purpose of this report the mechanism behind solar-like oscillations will be the main focus.

Within the stellar interior, radiation can be trapped due to the high opacity of the surrounding ionised material, a necessary property for stars driven by the κ mechanism. The build of radiation pressure causes the star to expand past the equilibrium radius until it eventually collapses again once the pressure is reduced, as the radiation can now escape.

Solar-like oscillators are stars that exhibit the same oscillation modes as the Sun. Their

placement on the HR diagram is shown in Fig.1. These stars are intrinsically stable and as a result the oscillations are not self-excited. The excitation of these modes is by the broad frequency range turbulence in the near surface convective regions of the star. This random excitation is known as the stochastic mechanism and is only present in stars with near surface convective zones. The stochastic mechanism can drive some waves towards resonance, whereas in others it can cause damping of the wave. As a result, the luminosity changes for solar-like oscillators are significantly smaller than that observed from other variables, such as κ mechanism oscillators. As a comparison, κ driven oscillators such as Cepheid variables show fractional luminosity variations of 10%, whereas solar-like oscillators have magnitude variations of parts per million.

Oscillations in Stars

Oscillation Modes

The two types of standing wave oscillations within a star are called g (gravity) and p (pressure) modes. In gravity modes the restoring force for the oscillation is the gradient of the gravitational acceleration within the star, they are also known as buoyancy waves. A parcel of gas within a star will rise if the material is less dense than of its surroundings. The g mode oscillations are present within the centre of stars as the rising parcel of gas will eventually become denser than its surroundings and will therefore sink. This continuous motion from the parcel of gas produces these g mode oscillations. A property of this motion is that there can be no pure radial motion, oscillation through the star centre, as the parcel of gas displaces surrounding material in all directions each cycle. g modes are observationally present within more evolved, or more massive, stars than that of the Sun.

In pressure modes the restoring force is the pressure gradient within the star. p modes are the acoustic waves excited by the stochastic turbulence of the near-surface convection zones. These acoustic oscillations can be trapped within a star setting up standing waves, resonances, that can be either radial, causing the star to periodically expand and contract keeping spherical symmetry, or non-radial, causing deviations from the spherical symmetry of the star. The oscillations can be described by spherical harmonics, with the parameters; l, m and n.

l is the angular degree of modes and describes the number of oscillation nodes on the stellar surface. Modes with different degree, l, is plotted on Fig. 2. It can also be used to give the horizontal wavelength, the wavelength that is parallel to the stellar surface from the sound waves, $\lambda_h = 2\pi R/L$ where $L = \sqrt{l(l-1)}$. Oscillations with an angular degree of l= 0 are radial modes, or fundamental modes, and those with l>0 are non-radial modes. l also indicates the depth at which the waves will penetrate too, where a lower value of l corresponds to a greater wavelength, thus a greater depth. Each value of l therefore probes a different cavity of the star, the size of which is the depth of the penetrating wave.

The azimuthal order m, gives a measure to the number of surface nodes that cross the stars equator. The value of m is given by -l<m <l. The frequencies of m are degenerate and are lifted by the rotation of the star. Oscillations with a velocity component in the rotation direction will be moving pro-grade, whereas oscillations with a velocity component against

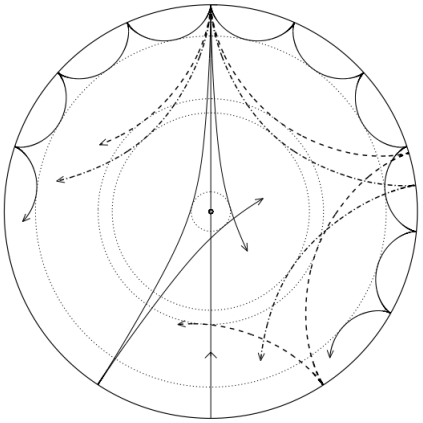

Figure 2: *Internal ray diagram of five p mode oscillations of various angular degree,* l. *The size of each cavity is dependent on the value of* l, *the modes represented are* $l = 0, 2, 20, 25$ & 75.[9]

the rotation direction will be moving retrograde. This advection causes the oscillations to be shifted to higher or lower angular frequencies, lifting the degeneracy. The magnitude of this effect can be shown by $\omega_{n,l,m} = \omega_{n,l,0} + \Omega m$, where Ω is an average value of the angular velocity within the cavity of which the waves are probing and ω is the angular frequency of the wave. This relation is subject to several approximations such as slow rotation of the star, small Coriolis force, and that the star remains spherical. Fast rotating stars can cause distortions that change the equilibrium of the star.

The radial order, n, or overtone number describes the total number of nodes in the radial direction. For solar-like oscillators, the frequencies observed suggest high overtone modes, and so the value of n is generally large. For the Sun, the frequencies that show the largest amplitudes have an overtone number of $n = 20$. Only low l modes are observed in unresolved stars due to geometric cancellation effects, with l=3 being the highest mode normally detected. In the Sun modes upto l=300 and in some case l=900 or higher. [5]

Frequency of Oscillations

Frequency of Maximum Power ν_{max}

The Frequency of maximum power, $\nu_{\max}$, is shown in Fig. 3.

Large Frequency Spacing $\Delta\nu$

It can be assumed that for the fundamental mode of a star, the mode that causes a star to expand and contract while keeping spherical symmetry, the acoustic time scale is equivalent to the dynamical time scale. The dynamical time scale for the Sun is given by $\tau_{dyn} \sim 1/\sqrt{G\langle\rho\rangle}$, where $\langle\rho\rangle$ is the mean density of the star. The period of this mode can be estimated from the time it takes the sound wave, τ , to travel across the stellar diameter, D. By relating the mean sound speed of the wave $\langle c\rangle$ to fundamental properties

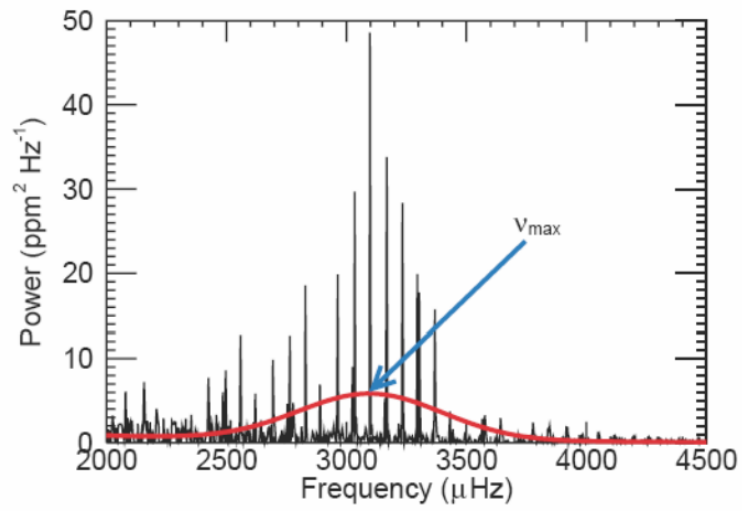

[H]

Figure 3: *Power spectra showing oscillation modes and fitted Gaussian envelope.* Original Chaplin et al. Ensemble Asteroseismology of Solar-Type Stars with the NASA Kepler Mission, 2009

of an ideal gas, the sound travel time $\tau \propto \langle\rho\rangle^{-0.5}$.

$$\nu_f = \frac{1}{\tau} = \frac{\langle c \rangle}{D} \propto \#langle\rho\rangle^{0.5} \tag{1}$$

For the Sun, the dynamical time scale is roughly one hour, giving a fundamental frequency of $\Pi = 2 \cdot \left(\frac{GM}{R^3}\right)^{-1/2}$ the inverse of which is $\approx 315\mu$Hz. However, observed pulsations from the Sun have periods of a few minutes, giving $\nu_f \approx 3000\mu$Hz. This would suggest that the observations are high overtones (high n) of the fundamental mode. These radial standing waves are analogous to the standing waves propagating within a 1-D pipe. The wavelength of overtone n within an open ended pipe is $\lambda = \frac{2R}{n+1}$, where R is the length of the pipe and as such, the radius of the star. We assume that the medium is homogeneous and that the edge effects are ignored, meaning that the overtones, n, see the same sized cavity. From this wavelength, the frequency of the fundamental and its overtones, the first harmonic and higher, can be given as $\nu_n = cn/2R$. This gives the definition of the large frequency spacing between these successive overtones $\nu = c/2R$. More formally the large frequency spacing is better represented by the following;

$$\Delta\nu = \left(2\int_0^R \frac{\mathrm{d}r}{c}\right)^{-1} \tag{2}$$

This 1-D pipe solution can also be generalised for the spherical geometry of a star. For a 3-D pipe, the waves will no longer be plane waves, and so there will also be an additional transverse component that moves at right angles to the radial axis, the non-radial modes. The transverse waves will have their own set of overtones and can be described with spherical harmonics.

The general form for a uniform non-rotating sphere is,

$$\nu_{n,l} = \Delta\nu_0(n + \frac{l}{2} + \epsilon) + \delta\nu \tag{3}$$

where η is a small factor of order unity, $\nu_{n,l}$ is the observed frequency at the given n and l, and $\Delta\nu_0$ is the large frequency separation. Equation 3 relies on an asymptotic relation for p modes that states that all modes are approximately equally spaced in frequency, assuming $n >> l$ [12]. The large frequency separation $\Delta\nu_0$ is the frequency difference between modes of the same l but consecutive radial order n, see Fig. 4.

Relation of $\Delta\nu$ to mean density $\langle\rho\rangle$

As Equation 2 shows, $\Delta\nu$ is related to the sound travel time across the star. This can easily be shown to relate the large frequency to the average density of the star, using the speed of sound in an ideal gas, and hydrostatic equilibrium. The sound speed is $c \propto \sqrt{P/\rho}$, where P is the pressure. Putting this back into the previous equation, and averaging over the radius R leads to,

$$\left(\Delta\nu \propto \sqrt{\frac{\langle\rho\rangle}{\langle P\rangle}} \cdot R\right)^{-1} \tag{4}$$

The next step is apply averages to the equation of hydrostatic equilibrium, remembering pressure decreases with increasing radius.

$$-\frac{\langle P\rangle}{R} \propto -\frac{M\langle\rho\rangle}{R^2} \tag{5}$$

Finally cancel factors of R and substitute in for mass and radius leads to the solution

$$\Delta\nu \propto \frac{1}{R}\sqrt{\frac{M}{R}} \propto \sqrt{\langle\rho\rangle} \tag{6}$$

Small Frequency Separation $\delta\nu$

The small separation (see Fig. 4) is defined as being the frequency difference between modes of same order n but differing in l by 2, e.g. $\delta\nu_{02}$ is the small frequency separation between modes $l = 0$ and $l = 2$. This is a key asteroseismic parameter, as it allows information to be extracted about compositional difference by radius in the star, and as such penetrate further than the photosphere. Since different l modes see different sized cavities and the lower l modes penetrate more deeply into the star, see figure 2, the frequency difference is caused by the travel time, and as such composition of the region the lower l mode sees. Since in general only $l = 0$ to $l = 2$ modes are detected in asteroseismology, in particular this can be used to probe the cores of these stars, since $l = 0$ will pass through the core, whilst $l = 2$ will be refracted before reaching the core. This ability to probe the core also allows the evolutionary state, and so age of the star to be explored. An important consequence of this is that stars that observationally are identical, such as evolved or evolving stars can be accurately described.

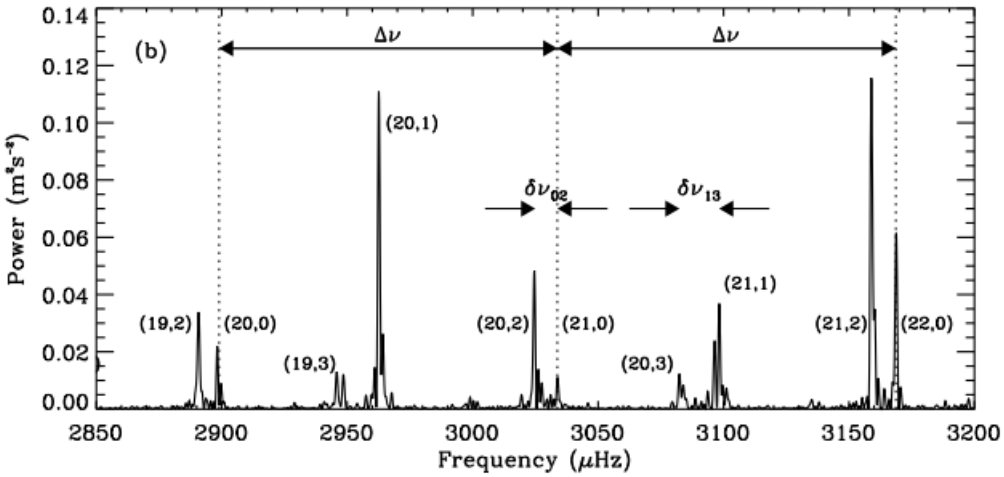

Figure 4: Zoomed power spectra showing with large $\Delta\nu$ and small $\delta\nu$ frequency spacings indicated. *Original Solar-like Oscillations: An Observational Perspective Bedding T.R., 2011*

Trapping Mechanism

Speaking of refraction, the trapping mechanism for oscillation modes should briefly be discussed.To obtain standing waves within a star, the waves must be trapped. Radial modes pass from one side of the star to the other by going through the star centre. Non-radial modes have a traverse direction where their anti-nodes are connected to the stellar surface, as shown in figure 2. The ray diagram shows two boundaries at which the wave is kept trapped in the star, these are the upper and the lower boundaries, detailing the reflection on the stellar surface and the refraction at some interior depth respectively. At the surface the sudden decrease in density causes waves lower than the acoustic cut-off frequency ν_{ac} to be trapped and reflected at the boundary. The lower boundary of the mode, caused by refraction, is due to the varying sound speed with depth, as $c \propto \sqrt{T}$ where T is the local temperature. This varying sound speed causes the wave to refract, defininig the lower boundary. Since the sound speed is also frequency dependent, different modes will penetrate to different temperatures, and so depths. [10]

Scaling Relations

Given these asteroseismic parameters, it is important to see what other stellar parameters can be extracted. Several parameters can be extracted using the relation in equation 6 and another standard relation, with all values normalised to solar values;

$$\frac{\Delta\nu}{\Delta\nu_\odot} = \sqrt{\frac{\rho}{\rho_\odot}}$$

,

$$\frac{L}{L_\odot} = \left(\frac{R}{R_\odot}\right)^2 \left(\frac{T}{T_\odot}\right)^4$$

This leads to the the scaling relation;[7]

$$\frac{L}{L_\odot} = \left(\frac{M}{M_\odot}\right)^{\frac{2}{3}} \left(\frac{T}{T_\odot}\right)^4 \left(\frac{\Delta\nu}{\Delta\nu_\odot}\right)^{-\frac{4}{3}} \tag{7}$$

however this relation will require an independent means to determine mass M, to allow the calculation of luminosity L and radius R. To do this another asteroseismic parameter extractable from the power, ν_{max}, the frequency of maximum power, which is central frequency of the gaussian modulating the spectra. A scaling relation for ν_{max} was found by Kjeldsen & Bedding 1995, which when combined with equation 6 leads to the final scaling relation to determine mass.

$$\frac{\nu_{max}}{\nu_{max,\odot}} = \frac{g}{g_\odot} \left(\frac{T_{eff}}{T_{eff,\odot}}\right)^{-0.5} \tag{8}$$

So far, an independent source for effective temperature has not been considered, but is generally established by spectroscopic measurement.

$$\frac{M}{M_\odot} = \left(\frac{\Delta\nu}{\Delta\nu_\odot}\right)^{-4} \left(\frac{\nu_{max}}{\nu_{max,\odot}}\right)^3 \left(\frac{T_{eff}}{T_{eff,\odot}}\right)^{1.5} \tag{9}$$

With these scaling relations and an independent source of T_{eff}, the project can progress, and power spectra, along with stellar parameters can be determined.

Analysis

We were given *Kepler* light curves for 10 stars, that are all solar-like oscillators and expected main-sequence (MS) stars. For each star we had one quarter of data, so 90 days. It is all short cadence, which means an integration time of ∼59 seconds. For each of the light curves obvious outliers were removed beforehand. We were not given the names of each star, so for clarity, we named them ourselves, perhaps in an unconventional way, but the translation from our names to the official names can be seen in the appendix. Figure 5 shows an example of one of the lightcurves that we worked with. This is for the star named Tina and as expected for a solar-like oscillator with low amplitude pulsations there is nothing to see except noise. We also chose to do the same analysis for a red giant that is also a solar-like oscillator.

Power Spectrum

The first step in analyzing time series is to perform a fourier transform in order to move the analysis to frequency domain instead of time domain. A fourier transform is fitting the time series with periodic functions, e.g. sine functions. The better the fit for the specific sine function, the more power that frequency will have. For this we use the program *Period04*, which is very simple to use and can calculate the fourier spectrum rather fast. For solar-like oscillators it is custom to plot the fourier spectrum as a power spectrum, which just means

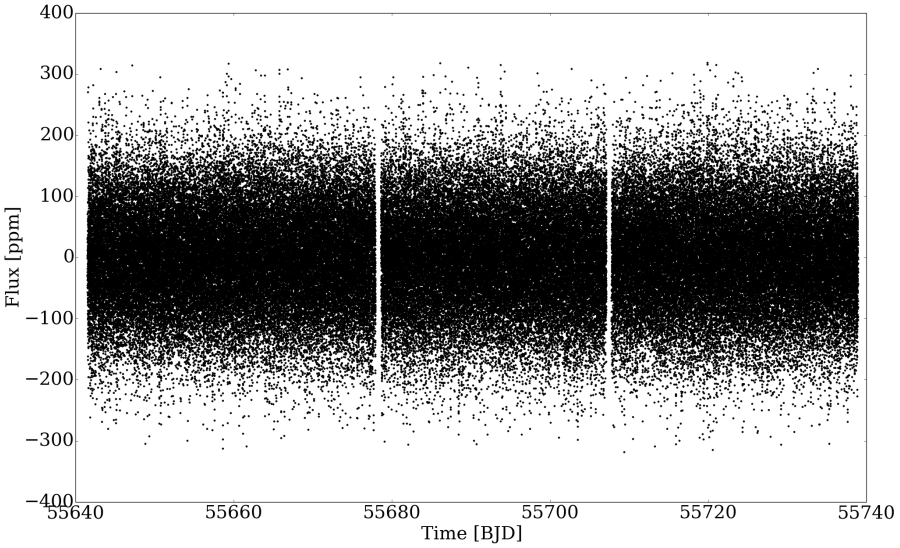

Figure 5: *Kepler lightcurve for Tina.*

that instead of amplitude vs. time, you plot power vs. time, where power is amplitude squared. It is also custom to use μHz instead of cycles/day. *Period04* plots the frequency in cycles/day and not μHz, so this is changed, when we do the further analysis with another program.

A fourier transform is a time expensive calculation, so it is worth considering how far up in frequency the transform has to go. The Nyquist frequency is the highest frequency that can contain relevant information. It is half the sampling frequency, which is the inverse of the time steps:

$$f_N = 1/2f_s = 1/(2\Delta T) \tag{10}$$

Everything above the Nyquist frequency will only be an alias of the information below the Nyquist frequency. Because our data is short cadence (short time steps) the Nyquist frequency is very high, $f_N \sim 1/(2 \cdot 59s) = 8474\mu$Hz, and it is not necessary to calculate the power spectrum all the way up to the Nyquist frequency. This would also take a very long time.

Figure 6 shows an example of a power spectrum. This is for the star named Jørgen. At low frequencies the granulation noise dominates. From $\sim 3000\mu$Hz and up there is no more information in this power spectrum. The excited modes are visible around 2165μHz. This frequency is called the frequency of maximum power, denoted as $\nu_{\max}$. We calculated this frequency by assuming a symmetrical distribution and then simply taking the average of the excited modes that we identified. This way of finding $\nu_{\max}$ is not so precise, but in general, $\nu_{\max}$ is not a very precise parameter and therefore we tried to avoid it in out analysis, but it was not always possible, see analysis section. If this analysis should be

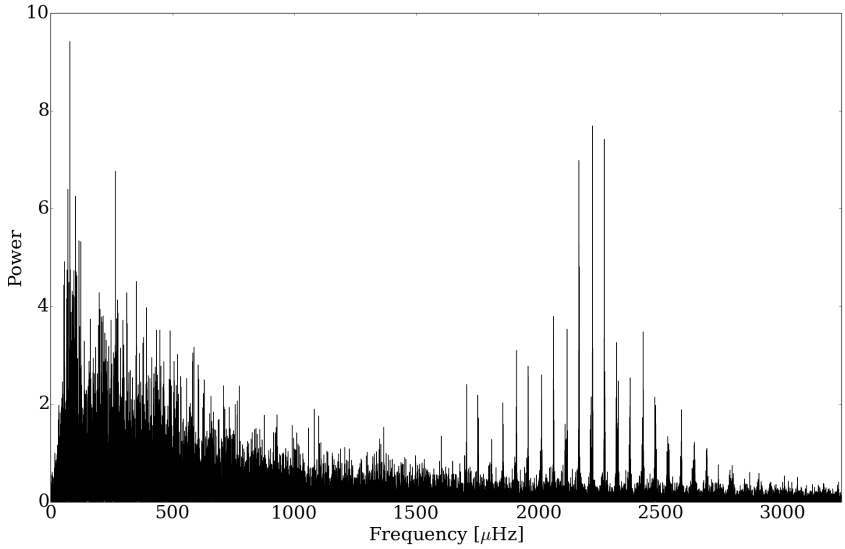

Figure 6: *A power spectrum for Jørgen.*

done more carefully, it would be a good approach to instead fit a gaussian envelope to the excited modes and thereby get the frequency of maximum power.

Echelle Diagram

The next step in the analysis is to determine the large frequency separation, $\Delta\nu$ and the small frequency separation, $\delta\nu$. As mentioned in the previous section, the large separation is the difference between two l=0 modes of consecutive radial order, n. The small separation is the different between the l=2 and l=0 mode of the same radial order. So first, we need to identify the modes. Figure 7 is a zoom around $\nu_{\max}$ for the star named Rhita. This star was the star, where the mode identification was easiest. For some of the stars it was much more difficult, which also adds a bigger uncertainty on the results. Two of each mode with different degree are marked, and the pattern clearly repeats. Period04 lets you choose each frequency for the modes you identify by simply clicking on the peak on the plot. For some of the stars however, the power spectra are not nearly as nice as that in Fig. 7. Figure 8 shows a zoom around the excited modes in the power spectrum for the star named Hans. Here, it was very difficult to determine the position of the center of the peaks by eye. To help aid the eye, we calculated the power spectrum with a lower resolution, which results in a smoothing of the spectrum, and this makes it easier to determine the center of the peak, but the precision is still much lower than for the nicer power spectra, e.g. for Rhita. If the analysis has to be more thorough and precise, it would be better to fit a Lorentzian profile to the peaks and with that determine the center of the peak.

To find $\Delta\nu$, we plot the frequency of l=0 modes of consecutive radial order, n. The slope is then the large frequency separation. This is then used to cut up the power spectrum

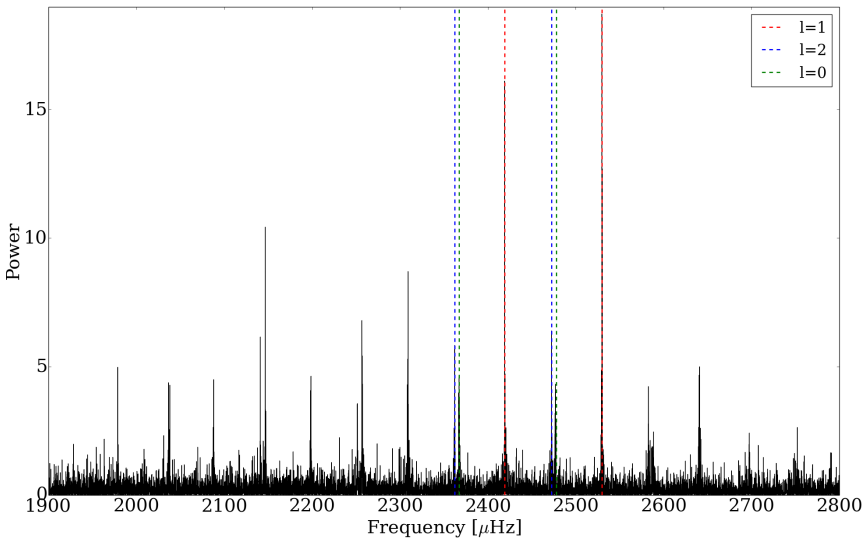

Figure 7: *A zoom around ν_{max} for Rhita. This shows the identification of two of each l=0, l=1 and l=2 mode.*

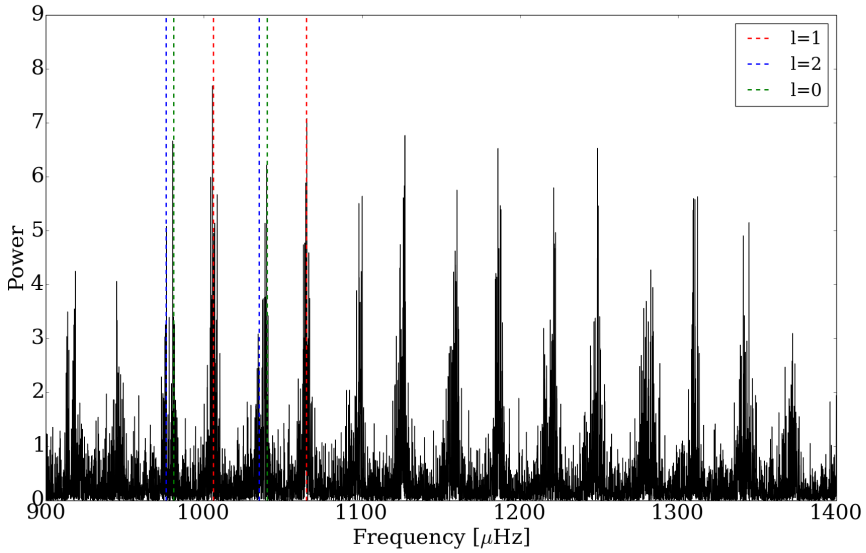

Figure 8: *A zoom around ν_{max} for Hans. As in Fig. 7, two modes of each degree is marked, but now the frequency of the center of the peak is a lot more difficult to determine.*

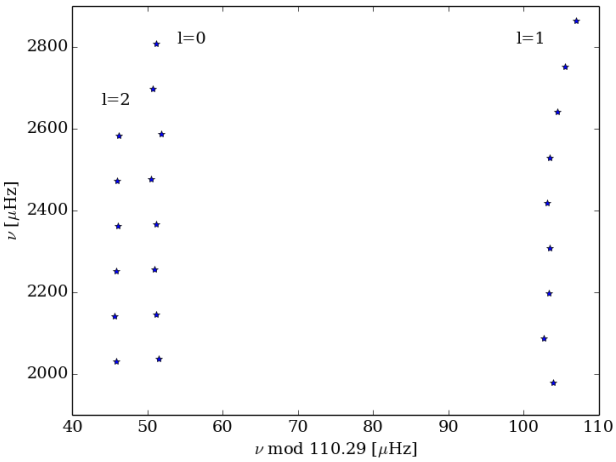

Figure 9: *The echelle diagram for Rhita, the 'nice' star.*

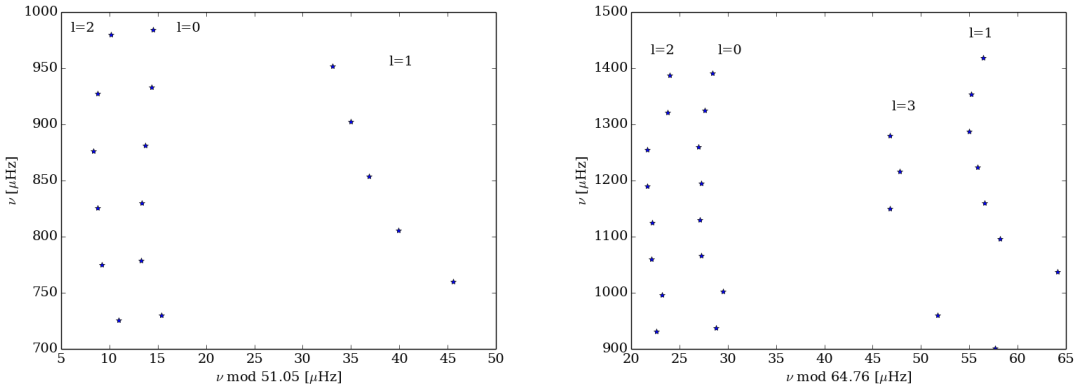

Figure 10: ***Left:*** *The echelle diagram for Frank with strange behaviour from the l=0 mode.* ***Right:*** *The echelle diagram for Vichi with three l=3 modes identified and the l=1 modes seems to be mixed.*

in equally sized pieces that is stacked on top of each other. This is called an echelle diagram, where the frequency is plotted against the frequency modulus the large frequency separation. An example for Rhita can be seen on the left in figure 9. This clearly shows the ridges that form by modes of same degree, l. This was the most well-behaved star we analyzed, two examples of less well-behaved stars is in Fig. 10. On the left is the echelle diagram for the star named Frank, where the l=1 mode shows some strange behaviour. On the right is the echelle diagram for the star named Vichi, where we were able to identify three l=3 modes and the l=1 mode seems to be mixed.

As mentioned before, the small frequency separation, $\delta\nu$, is the distance between the l=0 and l=2 modes. This can be determined from the echelle diagram. We calculated

Table 1: *Asteroseismic parameters for all stars. Brandon is the Red Giant star. The errors are only internal errors.*

Name	$\nu_{\max}$ (μHz)	$\Delta\nu$ (μHz)	$\delta\nu$ (μHz)	Literature $\Delta\nu$ (μHz)[1]
Hans	1131 ± 44	60.5 ± 0.1	5.4 ± 0.3	60.8 ± 0.2
Jørgen	2156 ± 8	103.7 ± 0.1	6.5 ± 0.4	104.3 ± 0.3
Kai	2258 ± 16	105.5 ± 0.1	7.9 ± 0.3	105.8 ± 0.3
Vichi	1148 ± 20	64.7 ± 0.1	$5.3 \pm 3.0{\cdot}10^{-2}$	65.1 ± 0.2
Rhita	2350 ± 41	$110.3 \pm 2.0{\cdot}10^{-3}$	$5.2 \pm 3.0{\cdot}10^{-3}$	110.1 ± 0.3
Frank	859 ± 5	$51.0 \pm 1.0{\cdot}10^{-2}$	4.8 ± 0.1	51.5 ± 0.2
Simon	3509 ± 46	149.2 ± 0.1	9.7 ± 0.2	149.1 ± 0.4
Tina	929 ± 11	53.3 ± 0.1	4.5 ± 0.2	54.0 ± 0.2
Regnar	1908 ± 18	88.8 ± 0.1	5.8 ± 0.2	87.9 ± 0.2
Karsten	1457 ± 14	$74.9 \pm 1.0{\cdot}10^{-2}$	5.1 ± 0.3	74.7 ± 0.2
Brandon	54 ± 1	5.5 ± 0.1	0.8 ± 0.2	5.5 ± 0.1

[1] Silva Aguirre et al (2012) and Chaplin et al (2013).

this in a very simple way, by just averaging the $\nu \mathrm{mod} \Delta\nu$ for the l=2 modes and for the corresponding l=0 modes of same radial order. Figure 9 and 10 shows how the precision on this also varies. For the nice star, Rhita, on Fig. 9, the small frequency separation between the l=0 and l=2 modes of same radial order, is very close to the same for all of them. For some of the stars, e.g. Frank and Vichi, on Fig. 10 $\delta\nu$ varies a bit more for different radial orders.

The results from this analysis is shown for all stars in Table 2. It is noteworthy that with our simple and rough approach to this analysis, we are still within 1% of the literature values for the large separation for most of the stars. This is compared to other groups who used more sophisticated methods, more data and also who have a much greater knowledge about asteroseismology than we do after one week.

Stellar parameters

The mass determination is possible with the C-D-Diagram (White et al., 2011). Here it is needed to plot the large seperation $\Delta\nu$ on the x-axis and the small separation, $\delta\nu$, on the y-axis. In Fig. 11 the C-D-diagram from White et al. (2011) is shown with the determined large and small separation for our stars (red dots), CoRoT stars (orange triangles), ground based observed stars (purple diamonds).

In the C-D-diagram, the stars evolve from top right to the bottom left. The C-D-diagram shows different isochrones which shows the mass and age of stars depending on the small and large separation. For five of the main sequence solar-like stars the determination of mass and age is possible, the other stars are much more evolved and the determination becomes more difficult. One of the red dots (the red giant star) is at the bottom left part of the diagram. The determination of the mass and age is difficult for sub giants and red giants. The problem occurs because of mode bumping for these types of stars. The evolving process of these stars leads to expanding their convective envelope and so the p-modes

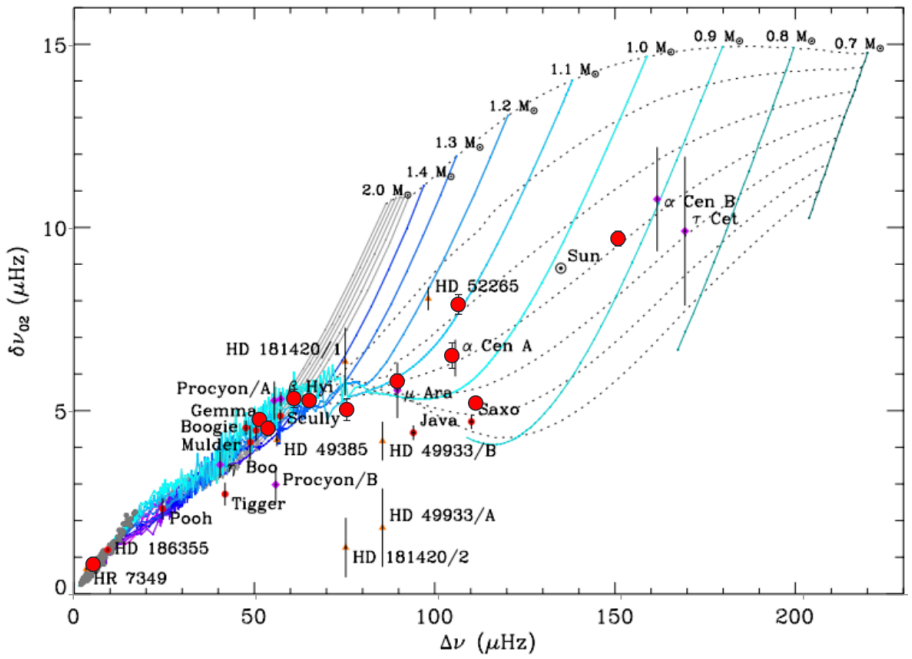

Figure 11: *C-D-diagram from White et al (2011) with our stars plotted as red dots.*

decrease in frequency and the g-modes increase in frequency and create mixed modes. This leads to high deviation from the asymptotic equation (1) and so to complications in the measurement of the small separation $\delta\nu$. The metallicity strongly affects the isochrones and the small and large separation. The C-D-diagram is made for near-solar metallicity. For smaller large and small frequency separations (which occurs for more evolved stars) it is no longer possible to accurately determine the mass and age from the C-D-diagram.

For the evolved stars, where the mass and age cannot be read off the C-D-diagram in Fig. 11, we can use an approximated equation from Chaplin & Miglio (2013) to determine the mass:

$$\frac{M}{M_\odot} = \left(\frac{\Delta\nu}{\Delta\nu_\odot}\right)^{-4} \left(\frac{\nu_{\max}}{\nu_{\max,\odot}}\right) \left(\frac{T}{T_\odot}\right)^{3/2} \tag{11}$$

For this we need the $\nu_{\max}$, which, as mentioned in the previous section, is more uncertain than the $\Delta\nu$ and $\delta\nu$, which makes this way of determining the mass less accurate. The age cannot be determined for these stars with the information we have available, and therefore these values are missing in Table... with the results.

After the mass has been read of the C-D-diagram or calculated using $\nu_{\max}$, the radius can be found using:

$$\frac{R}{R_\odot} = \left(\frac{\Delta\nu}{\Delta\nu_\odot}\right)^{-2/3} \left(\frac{M}{M_\odot}\right)^{1/3} \tag{12}$$

Table 2: *Stellar parameters for all stars.*

Name	T_{eff} (K)	M (solar)	Radius (solar)	Luminosity (solar)	Age (Gyr)
Hans	6270	1.4	1.92	5.1	
Jørgen	6060	1.1	1.22	1.8	5.8
Kai	6340	1.1	1.22	2.2	3.9
Vichi	5740	1.0	1.63	2.6	
Rhita	5720	1.0	1.13	1.2	9.6
Frank	6090	1.2	2.02	5.0	
Simon	5360	0.9	0.92	0.6	5.9
Tina	6200	1.3	2.02	5.4	
Regnar	6140	1.1	1.37	2.4	6.0
Karsten	6060	0.9	1.44	2.5	
Brandon	4620	1.4	9.59	37.7	

With this information, it is now possible to determine the luminosity of the stars:

$$\frac{L}{L_\odot} = \left(\frac{\Delta\nu}{\Delta\nu_\odot}\right)^{-4/3} \left(\frac{M}{M_\odot}\right)^{2/3} \left(\frac{T}{T_\odot}\right)^4 \tag{13}$$

For this we also need the temperature, which was given to us. The determined radius, mass, luminosity and age for few stars are listed in Table....

Our analyzed main sequence solar-like stars have an effective temperature of ~ 6000 K and $\sim 1M_\odot$. The radii differ from one solar radius to two solar radii. For some, the age could not be determined. In conclusion we now have mass, radius and luminosity and it is possible to plot our stars in a HR Diagram with the given effective temperatures: Some of our stars are G-type main sequence stars and some of them are evolved up the sub giant branch. The red giant is also clearly positioned on the red giant branch. One can see that our stars fits well into the HR-diagram. Qualitatively, this confirms that the determination of the properties of the analyzed stars was successful.

Conclusion

With asteroseismology it is possible to determine the mass, radius, luminosity and age of stars. In this work we used photometric data from the Kepler satellite for ten main sequence stars and one red giant to determine the stellar parameters by identifying the p-mode oscillations by hand. These modes allowed us to determine the large frequency separation, $\Delta\nu$, which is the inverse sound travel time across a stellar diameter and sensitive to the radius of the star, and the small frequency separation, $\delta\nu$, which is sensitive to the structure of the core composition and thereby also the age. The large and small separation was used to determine the mass and age of the main sequence stars using a C-D-diagram. For five main sequence stars it was possible to determine the mass and age. The other stars was too evolved to determine the mass and age with the C-D-Diagram. Instead we used the given approximation by Chaplin & Miglio (2013) to identify the mass using the

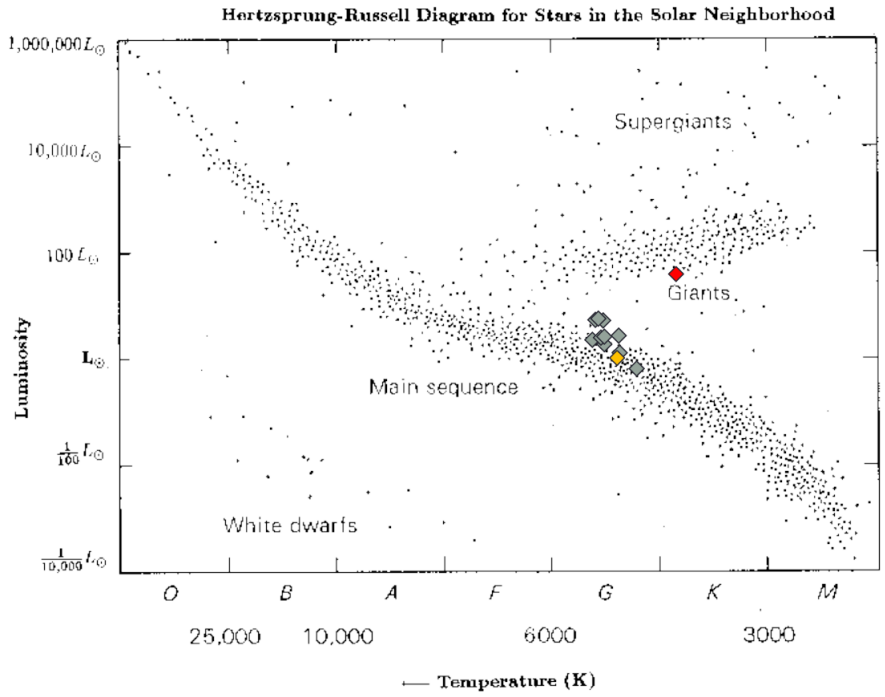

Figure 12: *HR diagram with our stars. The yellow diamond is the Sun, the red diamond is the red giant star and the grey diamonds are the 10 main sequence stars and sub giants.*

frequency of maximum power, $\nu_{\max}$. In the end we calculated the luminosity of the stars and plotted them in an H-R-diagram. Our results for the large separation (and following mass, age and radius) are in good agreement, within 1%, with results available in literature. The accurate determination of stellar parameters are important in order to understand the evolution of stars and moreover to determine more accurately the properties of celestial bodies around these stars, such as the characterisation of exoplanets.

Bibliography

[1] Bedding, T. R., 2011, ArXiv e-prints 1107.1723

[2] Chaplin, W. J. & Miglio, A., 2013, ARA&A, 51, 353

[3] White, T., et al. 2011, ApJ, 743, 161

[4] Silva Aguirre, V., et al. 2012, ApJ, 757, 99

[5] Birch A.C., *Current Issues in Helioseismology*, 2009

[6] Chaplin W.J., Lecture Notes: Insights into Stellar Structure, 2012

[7] Chaplin W.J., et al. Ensemble Asteroseismology of Solar-Type Stars with the NASA Kepler Mission. arxiv:1109.4723

[8] Cunha M.S., et al. AAR 14, 217, 2007

[9] Jørgen Christensen-Dalsgaard, Lecture Notes on Stellar Oscillations, Aarhus University, Fifth Edition, 2014

[10] Kjeldsen, H., & Bedding, T.R., Amplitudes of stellar oscillations: the implications for asteroseismology. A&A, 9403015, 1994.

[11] Kjeldsen, H. & Bedding, T. R. 1995, A&A, 293, 87, Paper I

[12] Kurtz D.W., *Stellar Pulsations: an Overview*, ASP Conference Series, Vol 349, 2006

Appendix

Table 3: *Name conversions.*

Name of files	KIC name	Our name
star0	KIC03632418	Hans
star1	KIC06106415	Jørgen
star2	KIC06225718	Kai
star3	KIC06442183	Vichi
star4	KIC06603624	Rhita
star5	KIC07976303	Frank
star6	KIC08006161	Simon
star7	KIC10068307	Tina
star8	KIC12009504	Regnar
star9	KIC12258514	Karsten
rgstar0	KIC02831788	Brandon